WIND AND WAVE INDUCED BEHAVIOUR OF OFFSHORE GUYED TOWER PLATFORMS

R. S. Bisht† and A. K. Jain*‡

†Consulting Engineering Corporation, 8490 A Tyco Road, Vienna, VA 22180, U.S.A.
‡Civil Engineering Department, Indian Institute of Technology, Hauz Khas, New Delhi 16, India

Abstract—Offshore guyed tower platforms belong to the group of compliant offshore platforms which are most suited for deep water exploration. The basic feature of compliant offshore platforms is that they are designed to move with the waves, in at least some degrees-of-freedom. As far as excitation of wave frequencies is concerned, the system opposes wave forces by inertial effects. The offshore guyed tower derives its stability against lateral movement from its mooring system.

In this study, the response of offshore guyed towers to random forces generated by wind and wave is investigated. The exposed portion of the tower is subjected to the action of turbulent wind, while the submerged portion is acted upon by random wave forces. The analysis includes the nonlinearities due to the Morison equation of drag force, the variable submergence effect due to waves, the instantaneous position of the tower and force excursion relation of the mooring lines. A parametric study is conducted to investigate the behaviour of the tower under waves, and the combined effect of wind and wave forces.

1. INTRODUCTION

The fundamental frequency of an offshore guyed tower is designed to be well below the frequency range of waves which are frequently encountered, and therefore it is very low. As a result, the guyed towers are susceptible to low frequency excitations. Since fluctuating components of the wind have significant energy at low frequencies, such towers may have significant dynamic response due to gustiness of wind. The magnitude of the wind induced vibration depends upon the length and area of the exposed portion of the tower and the wind velocity.

The wind induced vibration of offshore guyed towers is complicated due to the fluid–structure interaction produced by the combined effect of random wind and wave forces. As such, very little literature is available on the wind induced vibration of compliant platforms (Smith, 1990; Ansari, 1991; Vickery, 1990; Qi *et al.*, 1991).

In this paper, the response of an offshore guyed tower to random forces, generated by the combined action of wind and wave, is investigated. The exposed portion of the tower is subjected to the action of turbulent wind, while the submerged portion is subjected to random (wind driven) wave forces. The two random phenomena are assumed to be statistically independent (i.e. no correlation exists between the two). The response analysis is performed by the iterative frequency domain procedure. Nonlinearities considered in the analysis are due to the Morison equation of drag force, variable submergence effect due to waves, and the force excursion relation of the mooring lines. A parametric study is conducted to investigate the dynamic behaviour of the tower under wave (wind driven) forces and the combined effect of wind and wave forces.

2. ANALYSIS

2.1. *Equation of motion*

A prototype offshore guyed tower (Fig. 1(a)) has been considered for the present study. The tower has been idealized as a uniform shear beam with a rotational spring at the base of the tower (Fig. 1(b)). The guylines have been idealized by a nonlinear spring. The stiffness of the nonlinear spring is obtained from a separate static analysis of the guylines under its own weight. The typical force excursion relationship of 20 guylines is shown in Fig. 1(c). For the combined wind and wave loading, the equations of motion, in structural coordinates, take the form

$$[M]\ddot{X} + [C]\dot{X} + [K]X = F(t) = F_{\rm h}(t) + F_{\rm w}(t) \qquad (1)$$

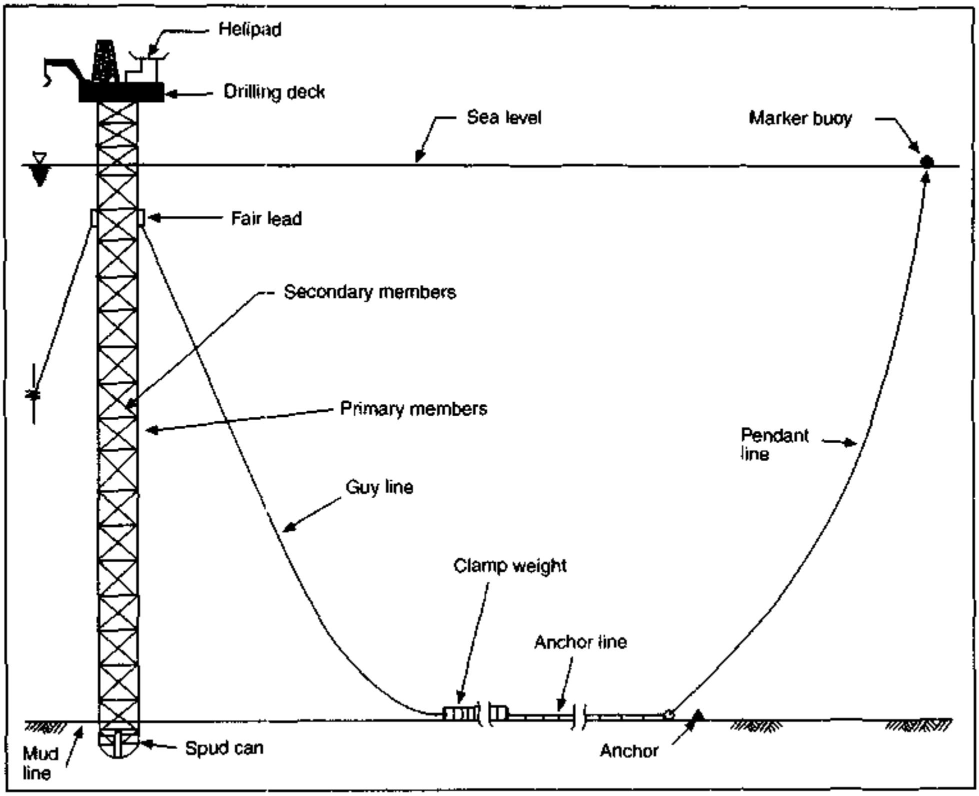

(a)

Fig. 1. (a) Schematic of prototype guyed tower. (b) Finite element model of guyed tower. (c) Force excursion relationship (20 cables).

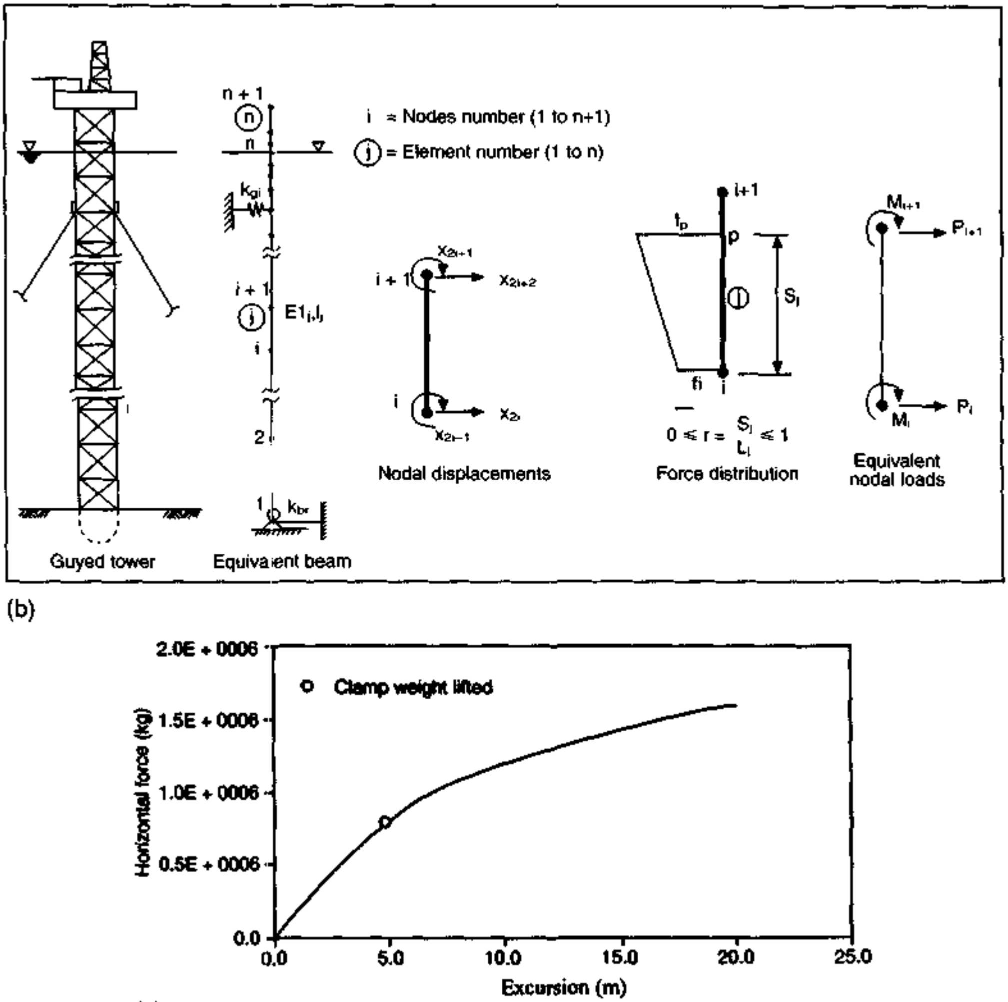

Fig. 1. Continued.

where $[M]$ is the time invariant diagonal mass matrix having lumped masses and rotatory inertia of elements at nodes. In the submerged portion of the tower, the effect of added mass up to mean sea level is taken in $[M]$. $[K]$ is generated by directly assembling the stiffness matrix for the elements, each having four degrees-of-freedom consisting of translations and rotations at the ends. $[C]$ is assumed as a linear combination of $[M]$ and $[K]$, so that ζ can be used directly in the equation of motion when uncoupled. $F_h(t)$ is the hydrodynamic load, $F_w(t)$ is the wind load acting on the exposed portion of the tower.

2.2. *Wind load*

On the exposed portion of the tower, the dynamic wind force is produced by the fluctuating component of the wind velocity. The tower is subjected to a drag force caused by the wind velocity normal to the tower. The drag force per unit length at node i of the tower is given by

$$f(t) = 0.5\bar{C}_d\rho_w DU_{ni}^2 \tag{2}$$

in which $\bar{C}_d$ is the wind drag coefficient, D is the equivalent wind drag diameter, U_{ni} is the total wind velocity at node i normal to the tower, and ρ_w is the mass density of wind. U_{ni} has two components, i.e. a steady mean wind velocity $\bar{V}_{ni}$ and the fluctuating component U_{ni}. The dynamic force is caused by the latter. Thus, the dynamic component of the wind force is given by

$$\bar{f}_{di} = \bar{C}_d\rho_w D(\bar{V}_{ni}u_{ni} + 0.5u_{ni}^2) \tag{3}$$

However, in the wind force $F_w(t)$ in Equation (1), the steady part of the wind force is also retained. This is done to obtain the total mean response directly from the analysis and to duly consider the effect of total displacement of the tower in the evaluation of wave (hydrodynamic) load using Morison's equation.

The wind force over an element is assumed to vary linearly between two nodes. The load is obtained for all the exposed members above the water level.

The fluctuating component of the wind velocity is random in nature and is simulated for a given wind velocity spectrum. Davenport's wind velocity spectrum (Davenport, 1961), as given below, is used in this study:

$$\frac{nS(z, n)}{\bar{V}^2(10)} = \frac{0.2x^2}{(1 + x^2)^{4/3}} \tag{4}$$

where $x = 1200n/\bar{V}(10)$, in which n is the frequency (Hz); $\bar{V}(10)$ is the mean wind speed (m/s) at height $z = 10$ m; $S(z, n)$ is the ordinate of the wind velocity spectrum [(m/s)^2/Hz].

To calculate the wind forces (along the height of the tower), the mean wind velocity along the height is calculated according to the following power law (Simiu and Scanlan, 1978):

$$\bar{V}(z_1) = \bar{V}(z_2)\left(\frac{z_1}{z_2}\right)^{\alpha} \tag{5}$$

The value of α for open terrain is used here, taken equal to 0.16 (Simiu and Scanlan, 1978). The wind velocities are assumed to be fully correlated along the height of the exposed portion of the tower. Thus, the time histories of wind velocity at different heights can be generated with the help of the wind velocity spectrum defined by Equation (4), and using the Monte-Carlo simulation procedure suggested by Goda (1970).

2.3. *Wave load*

The time histories of the water particle kinematics have been evaluated using the Pierson–Moskowitz spectrum (Pierson and Moskowitz, 1964) and Monte-Carlo simulation procedure (Goda, 1970). A random wave is represented by the Pierson–Moskowitz (wind driven) spectrum, given as

$$S_{\eta\eta}(\omega) = \left(\frac{Ag^2}{\omega^5}\right)\exp\left\{-B\left(\frac{\omega_0}{\omega}\right)^4\right\} \tag{6}$$

where $A = 0.0081$; $B = 0.74$; $\omega_0 = g/\bar{U}_{ni}$.

$\bar{U}_{ni}$ is the mean wind velocity at a height of 19.5 m above the MSL. The mean wind velocity $\bar{U}_{ni}$ at a height of 19.5 m is obtained from that at the reference height of 10 m by using the power law (Equation (5)) with 0.16 as the power coefficient. Equation (6) is used to simulate the four sea states corresponding to mean wind velocities of 10, 15, 20 and 25 m/s at a height of 10 m above mean sea level. The linear Airy's wave theory with Chakrabarti's modifications (Chakrabarti, 1971) has been used, in order to incorporate the effect of variable submergence due to waves. The wave load intensity is evaluated using the Morison equation for flexible structures:

$$f(t) = 0.5\rho C_d D_d(\dot{u} - \dot{x})|(\dot{u} - \dot{x})| + \frac{\pi}{4}\rho D_i^2 C_m \ddot{u} - \frac{\pi}{4}\rho D_i^2 (C_m - 1)\ddot{x} \tag{7}$$

where ρ is the mass density of sea water; C_d and C_m are drag and inertia coefficients, respectively; D_d and D_i are effective drag and inertia diameters, respectively. The equivalence of drag and inertia diameters for the cylinder is found from actual drag and inertia forces in each elemental zone of the real structure; $\dot{u}$ and $\ddot{u}$ are the normal water particle velocity and acceleration, respectively, and $\dot{x}$ and $\ddot{x}$ are structural velocity and acceleration, respectively. The last term in Equation (7) is to account for the change in added mass from mean sea level position, since the added mass up to mean sea level has already been accounted for in $[M]$.

2.4. *Iterative frequency domain solution*

For a specified time length of the simulated time histories of the wind and wave forces, the responses are obtained using the iterative frequency domain technique as described by Jain and Datta (1990). The present solution, in addition, treats the nonlinear restoring force due to guylines in the right-hand side load vector. Therefore, the solution technique is presented in brief. Equation (1) can be transformed as

$$\psi_p = \left\{\frac{\psi_{pc}}{\psi_{ps}}\right\} = 0 \quad p = 1,\ldots,n \tag{8}$$

in which

$$\psi_{pc} = [K - (p\sigma)^2 M]X_{pc} - (p\sigma)CX_{ps} - F_{pc} \tag{9}$$

$$\psi_{ps} = (p\sigma)CX_{pc} + [K - (p\sigma)^2 M]X_{ps} - F_{ps} \tag{10}$$

where ψ_p is a vector of order $4N$, ψ_{pc} and ψ_{ps} are of order $2N$; N being the total number of nodes and $2N$ being the total number of degrees-of-freedom; X_{pc}, F_{ps}, etc. are components of the Fourier transform of $X(t)$, $F(t)$, etc. In general, the load vector $F(t)$, consisting of wind and wave forces, is expressed as

$$F(t) = K^d S + K^m \ddot{U} + K^R x_g \tag{11}$$

in which K^d and K^m are the drag and inertia coefficient matrices of order $(2N \times N)$, respectively, and K^R is a $(2N \times 2N)$ diagonal matrix having non-zero value only at the gth diagonal element; the gth row corresponds to the translational degree-of-freedom at the node where the guyline is attached; x_g is the displacement at the guyline attachment point; S and $\ddot{U}$ are vectors of order N, where

$$S_j = |V_j(t)|V_j(t) \tag{12}$$

The relative velocity is defined by

$$V_j(t) = \dot{u}_j - \dot{x}_j \tag{13}$$

Since the hydrodynamic loading (Morison's equation) is dependent on the structural velocity and displacement, solution of Equation (8) requires iteration. In order to make the iteration scheme computationally less expensive, the Jacobian in the Newton–Raphson scheme is evaluated approximately by ignoring the derivatives of the pth harmonic of the nodal loads with respect to the qth harmonic of any of the nodal displacements ($q \neq p$) as a first approximation. With this approximation, the equation for the rth iteration becomes

$$J^r_{pp} X^r_p = J^r_{pp} X^{r-1}_p - \psi^r_p \tag{14}$$

in which ψ_p is the function defined by Equation (8); the superscript r describes the iteration number; J_{pp} is a $(4N \times 4N)$ Jacobian matrix given by

$$J_{pp} = \frac{\partial \psi_p}{\partial X_p} = \bar{K}_p - \bar{F}_p \tag{15}$$

The $\bar{F}_p$ matrix can finally be put in the following form:

$$\bar{F}_p = \begin{bmatrix} -K^d\{D^r_{cc} \vdots 0\}2p\sigma + K^R & K^d\{D^r_{cs} \vdots 0\}2p\sigma \\ -K^d\{D^r_{sc} \vdots 0\}2p\sigma & K^d\{D^r_{ss} \vdots 0\} + K^R \end{bmatrix} \tag{16}$$

in which D_{cc}, D_{cs}, D_{sc} and D_{ss} are all diagonal matrices of order N; their jth elements are, respectively, R_{sj}, $(R_{oj} + R_{cj})$, $(R_{oj} - R_{cj})$, R_{sj}, in which R_{oj}, R_{cj} and R_{sj} are given by

$$R_{oj} = \frac{1}{T} \int_0^T |V_j(t)| \, dt \tag{17a}$$

Table 1. Details of the idealised offshore guyed tower and hydrodynamic data

Deck height	480.1 m
Height at guy node	442 m
Guy diameter	9 cm
Number of guy lines	20
Guy initial tension	167,800 kg/m
EI	5×10^{12} kgm^2
Deck weight	693576 kg
Structural weight	3794 kg/m
Base restraint	22×10^8 kgm/rad
Structural damping, ζ	2%
Structure's first frequency	0.2689 rad/s
Structure's second frequency	1.3260 rad/s
Mean sea level	457.20 m
Effective drag diameter	35.05 m
Effective inertia diameter	5.79 m
C_d	0.9
C_m	2.0
Equivalent wind drag diameter	15 m

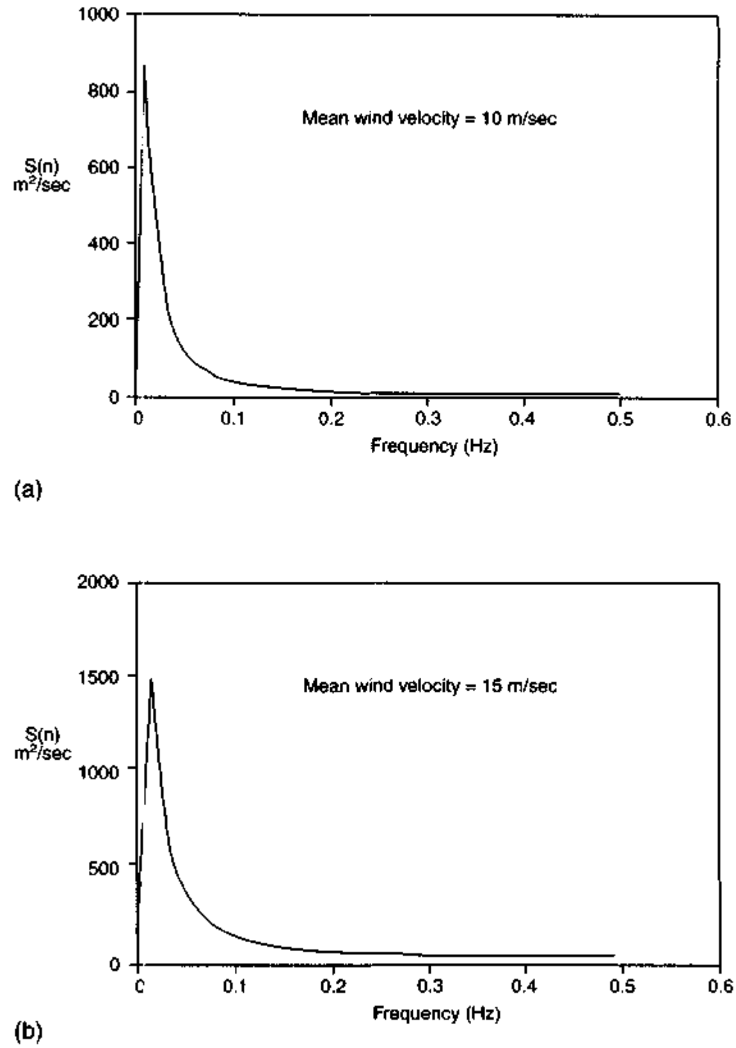

Fig. 2. Wind velocity spectra.

$$R_{cj} = \frac{1}{T}\int_0^T |V_j(t)| \cos(2p)\sigma t \,\mathrm{d}t \tag{17b}$$

$$R_{sj} = -\frac{1}{T}\int_0^T |V_j(t)| \sin(2p)\sigma t \,\mathrm{d}t \tag{17c}$$

Substituting Equations (9), (10) and (15) into Equation (14), the iteration equation becomes

$$\bar{K}_p X_p^r - \bar{F}_p X_p^r = F_p^r - \bar{F}_p X_p^{r-1} \tag{18}$$

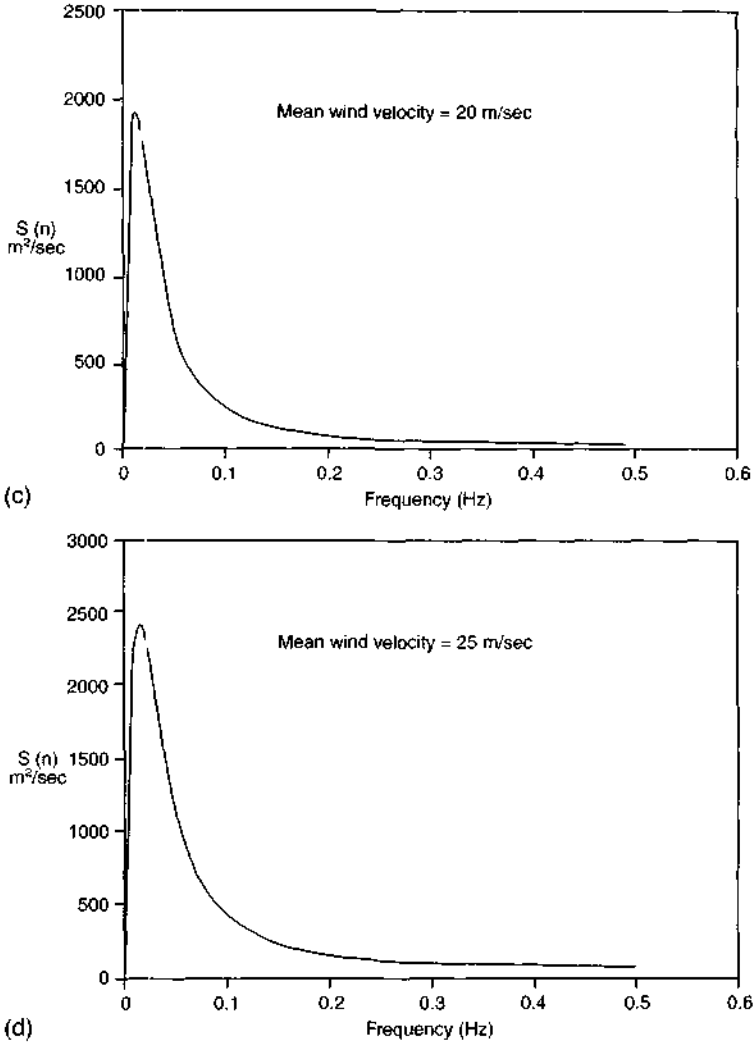

Fig. 2. Continued.

Examination of Equation (18) reveals that the second term on either side of the equation acts as a damping force. The efficiency of the solution depends upon how the term $\bar{F}_p$ is evaluated. Assuming R_{cj} and R_{sj} are zero, $\bar{F}_p$ takes the form

$$\bar{F}_p = 2(p\sigma)\begin{bmatrix} \dfrac{K^R}{2(p\sigma)} & K^d\{D^r_{cs}:0\} \\ -K^d\{D^r_{sc}:0\} & \dfrac{K^R}{2(p\sigma)} \end{bmatrix} \tag{19}$$

The computation of $\bar{F}_p$ involves only the computation of the time average of $|V_j(t)|$ for each node. In order to facilitate the computation further, normal mode theory is used. Once X_{pc} and X_{ps} are obtained in a particular iteration cycle, these are used to evaluate the loading functions for the next iteration until convergence is achieved with a specified tolerance limit.

3. NUMERICAL STUDY

Numerical studies are carried out to investigate the responses due to: (i) wave only and (ii) wind and wave acting together. The details of the idealized offshore guyed tower model adopted for the present investigation are given in Table 1. For the wind velocity spectrum, four values of mean wind velocity (at the reference height of 10 m) are con-

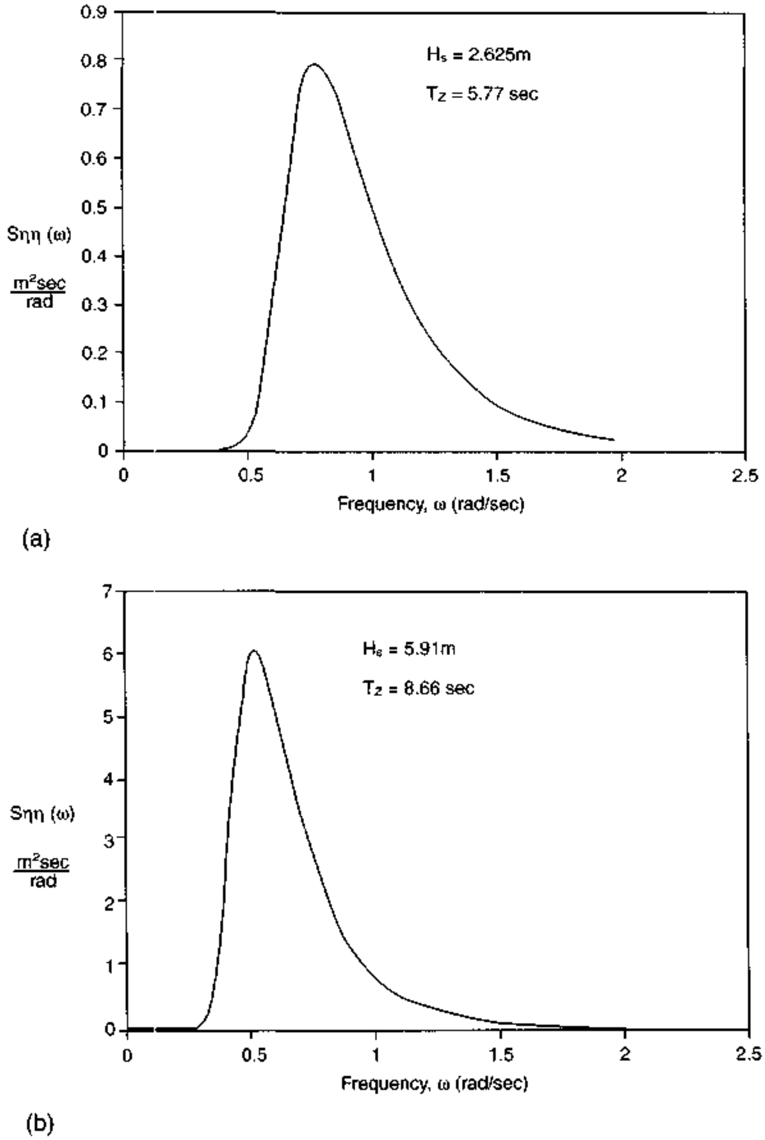

Fig. 3. Sea surface elevation spectra.

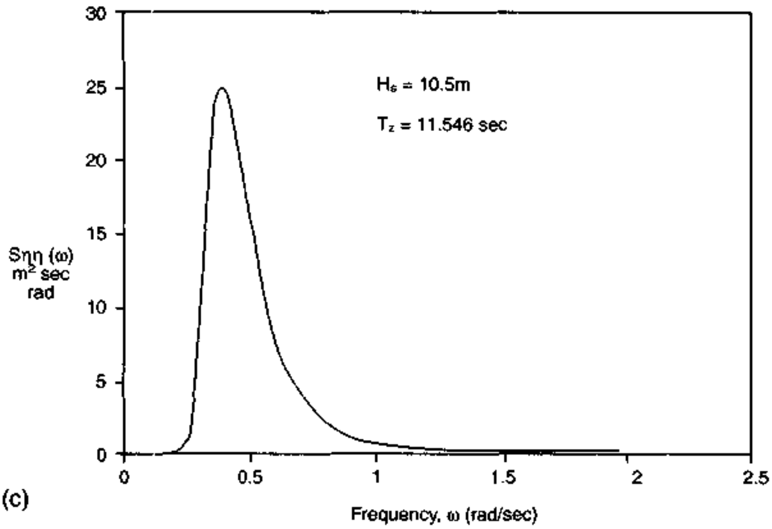

(c)

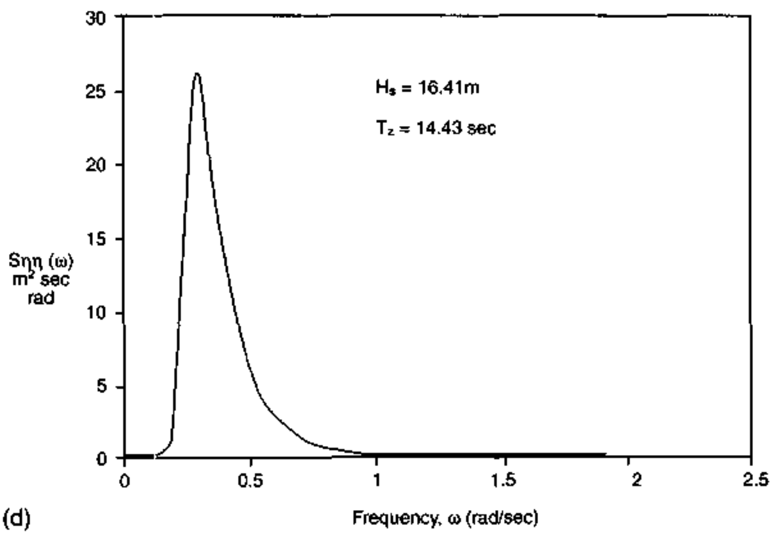

(d)

Fig. 3. Continued.

sidered, i.e. 10, 15, 20 and 25 m/s. The exposed height of the tower is 23 m. The equivalent wind drag diameter for the wind force calculation is taken as 15 m. This value has been derived on the basis of equivalent cylindrical exposed area available for wind exposure from the actual structural configuration of 23 m height. The recording time length T for the simulated time histories is taken as 1024 s, with a sampling interval of 0.5 s. The realised wind velocity spectra from the simulated wind velocity time histories are given in Fig. 2(a)–(d) for the four mean wind speeds. The *P–M* spectra for the sea surface elevation are given in Fig. 3(a)–(d).

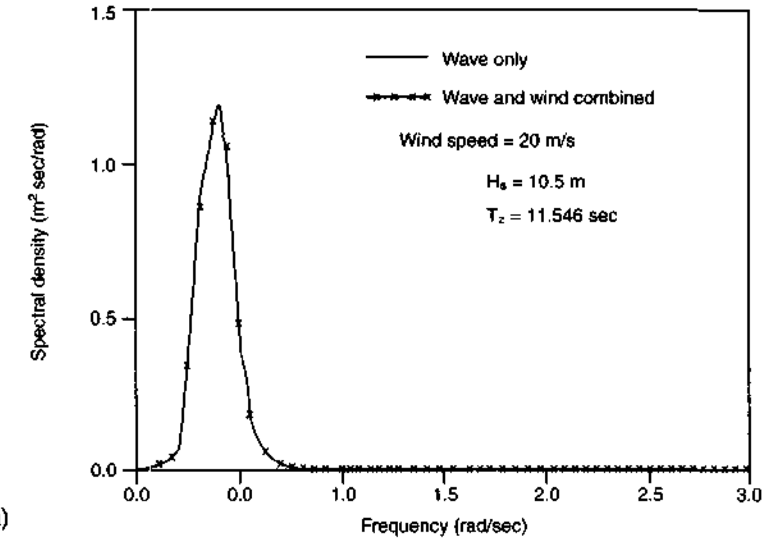

(a)

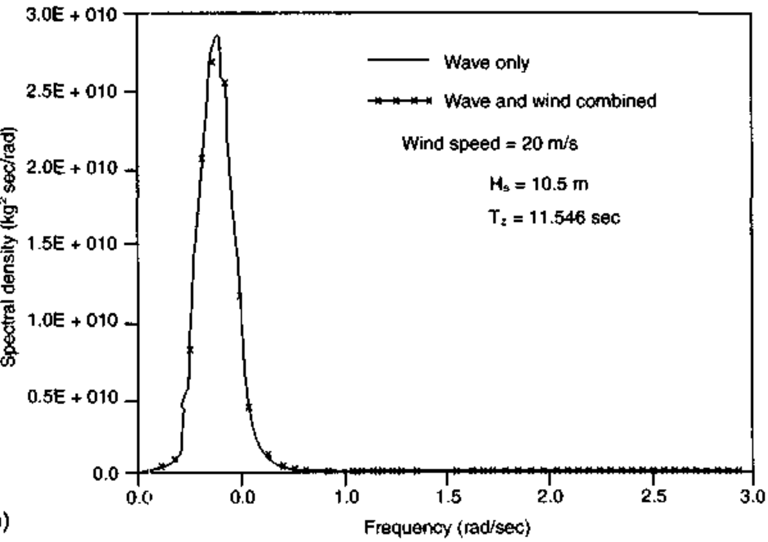

(b)

Fig. 4. (a) PSDF of tip displacement due to wind and wave forces. (b) PSDF of guy force due to combined wind and wave forces. (c) PSDF of bending moment, due to wind and wave forces, at guy node. (d) PSDF of shear force, due to wind and wave forces, at guy node.

Fig. 4(a)–(d) shows the Power Spectral Density Functions (PSDFs) of responses for waves (10.5 m/11.546 s) and combined action of wind and wave for a mean wind velocity of 20 m/s. The PSDF of tip displacement and guy force are characterised by a single peak occurring at 0.39 rad/s (the significant frequency of the sea spectrum). Thus, the energy contents of the sea spectrum predominantly governs the nature of the responses; the effect of the fluctuating component of the wind on the response is insignificant. This is also evident from the fact that the PSDF of responses for waves and the combined action of

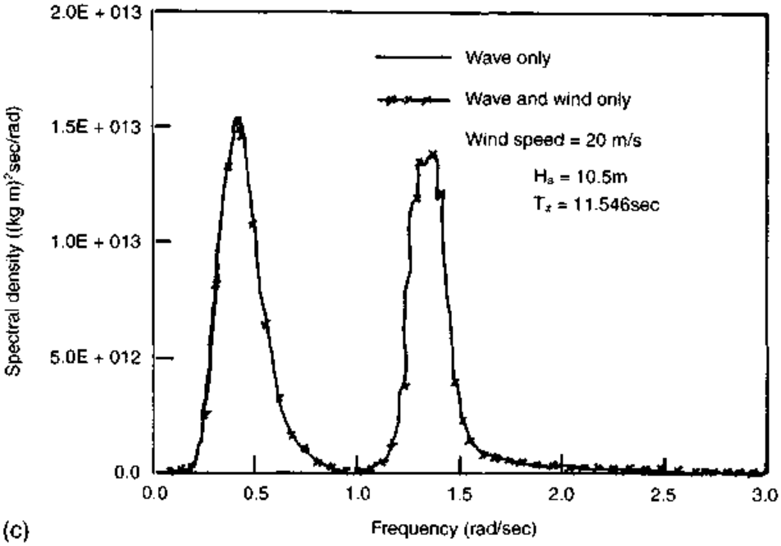

(c)

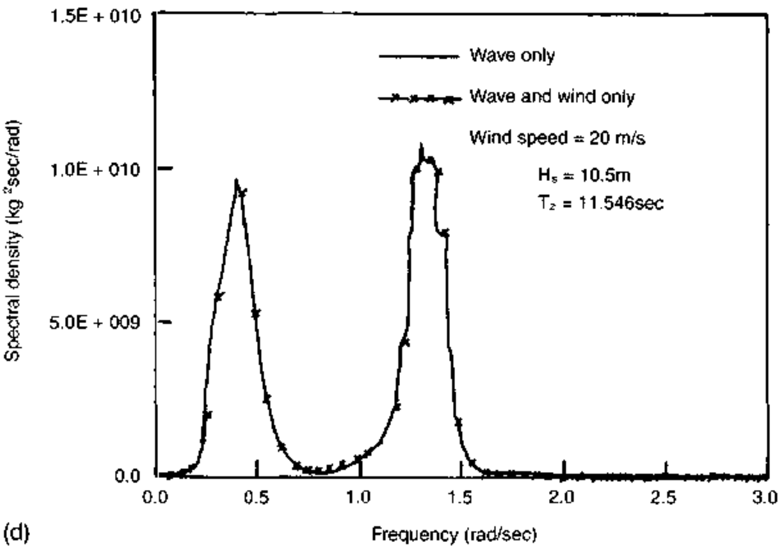

(d)

Fig. 4. Continued.

wave and wind are nearly the same. The behaviour due to the mean wind velocity of 25 m/s and the corresponding wave (16.4 m/14.43 s) has been found to be similar to the 20 m/s mean wind velocity case.

The PSDFs of bending moment and shear forces at the guy node (Fig. 4(c)–(d)) are characterised by two peaks. The second peak occurs at the structure's second frequency, and is as significant as the first one. This is due to the fact that the second mode contributes significantly to the bending response of the tower and the combined wind and wave force has significant energy content at the structure's second frequency.

Fig. 5(a)–(d) shows the PSDFs of responses for waves (5.91 m/8.66 s) and the combined action of wind and wave for a mean wind velocity of 15 m/s. The PSDFs of tip displacement and guy force are characterised by three peaks. The first peak (also the highest one) occurs at the structure's fundamental frequency, the second and third peaks occur, respectively, at the significant wave frequency and the structure's second frequency. The response PSDFs clearly indicate that the wave forces due to the 5.91 m/8.66 s wave have significant energy contents, both at the structure's fundamental and second frequency.

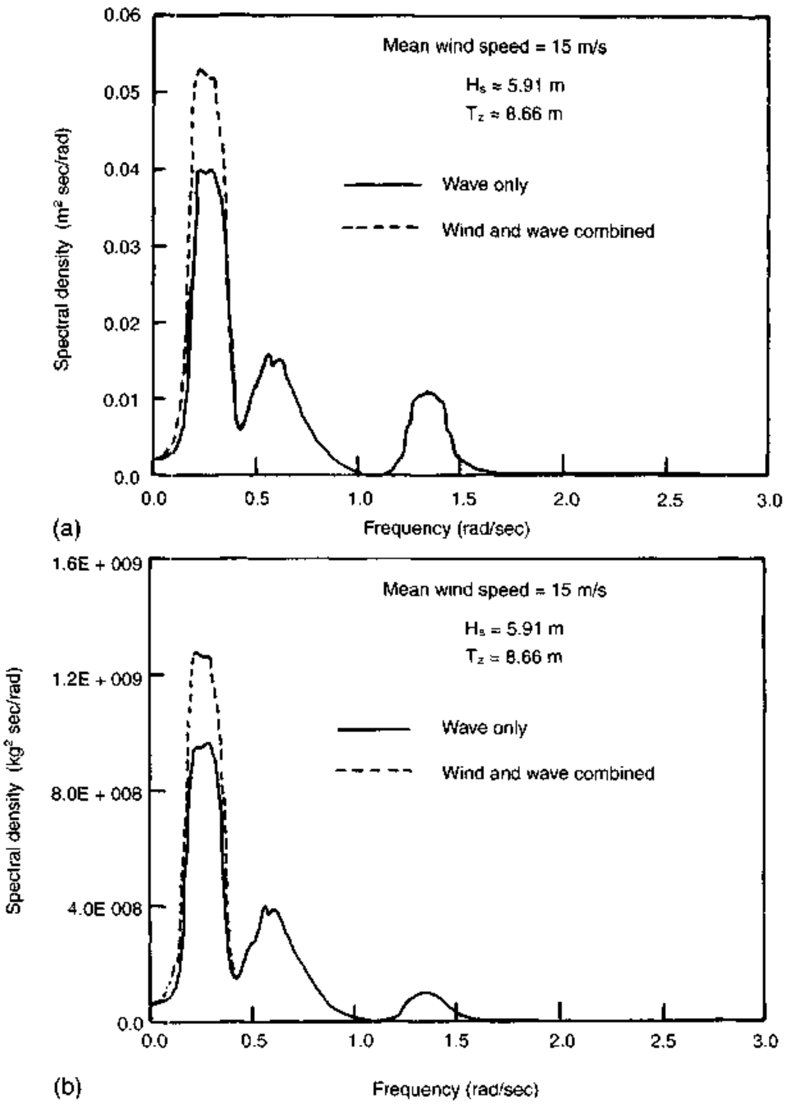

Fig. 5. (a) PSDF of tip displacement due to combined wind and wave forces. (b) PSDF of guy force due to combined wind and wave forces. (c) PSDF of bending moment, due to combined wind and wave forces, at guy node. (d) PSDF of shear force, due to combined wind and wave forces, at guy node.

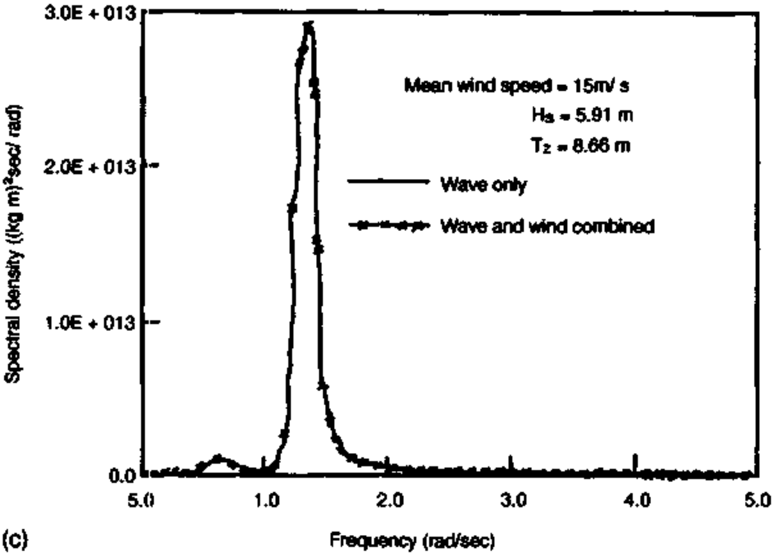

(c)

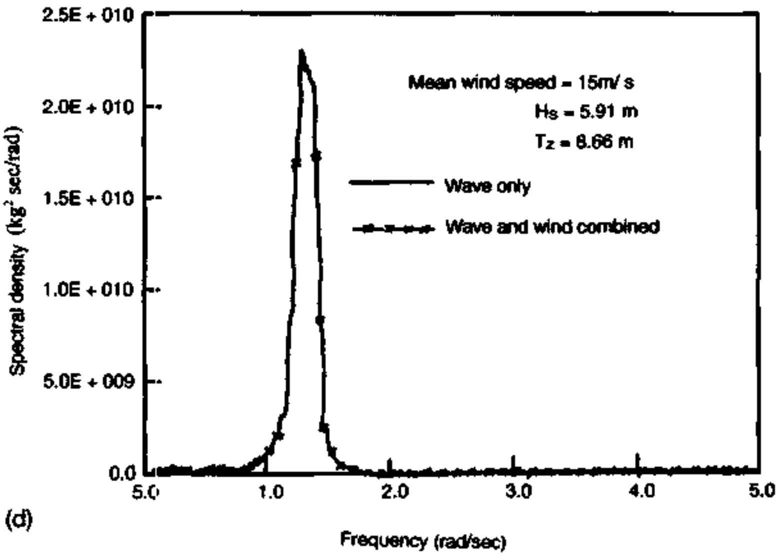

(d)

Fig. 5. Continued.

Further, the energy content at the fundamental frequency is enhanced for the combined wind and wave forces. As a result, the peak of the PSDF at the structure's fundamental frequency is increased for the combined action of wind and wave forces. Fig. 5(c) and (d) shows the PSDF of bending moment and shear force at the guy node. The PSDFs are characterised by a single peak occurring at the second frequency of the structure. Since wind force has insignificant energy content at higher frequencies, therefore it does not contribute much to the bending response.

Fig. 6(a)–(d) shows the PSDFs of responses for waves (2.625 m/5.77 s) and the combined action of wind and wave forces for a mean wind velocity of 10 m/s. The nature of the PSDF is similar to that observed for 15 m/s wind velocity. The only difference is that the effect of wind in modifying the response PSDFs at the structure's fundamental frequency is considerably more.

Table 2 shows the mean and standard deviation of the response quantities for various

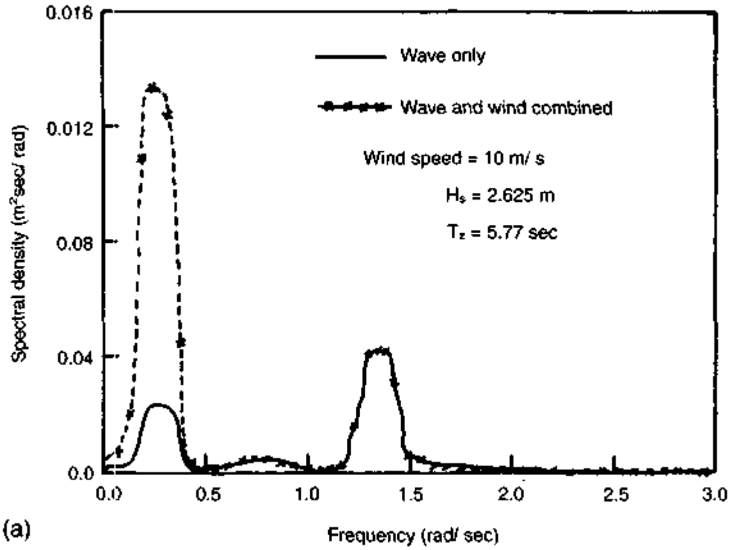

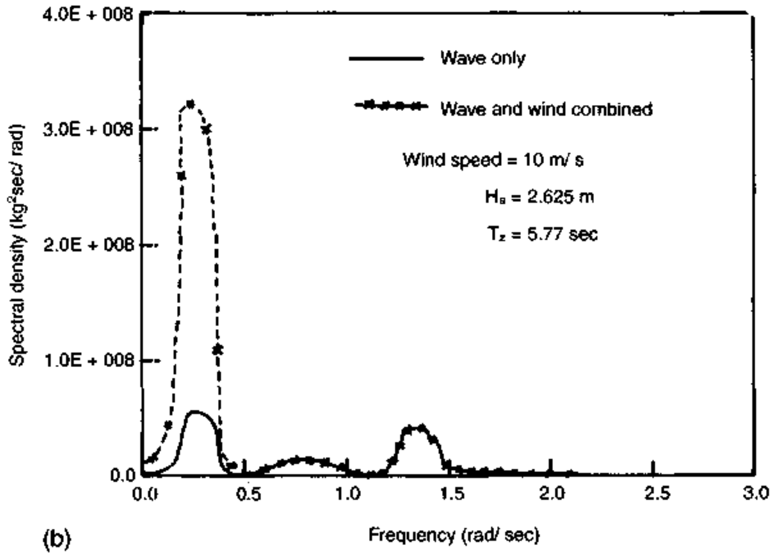

Fig. 6. (a) PSDF of tip displacement due to combined wind and wave forces. (b) PSDF of guy force due to combined wind and wave forces. (c) PSDF of bending moment, due to combined wind and wave forces, at guy node. (d) PSDF of shear force, due to combined wind and wave forces, at guy node.

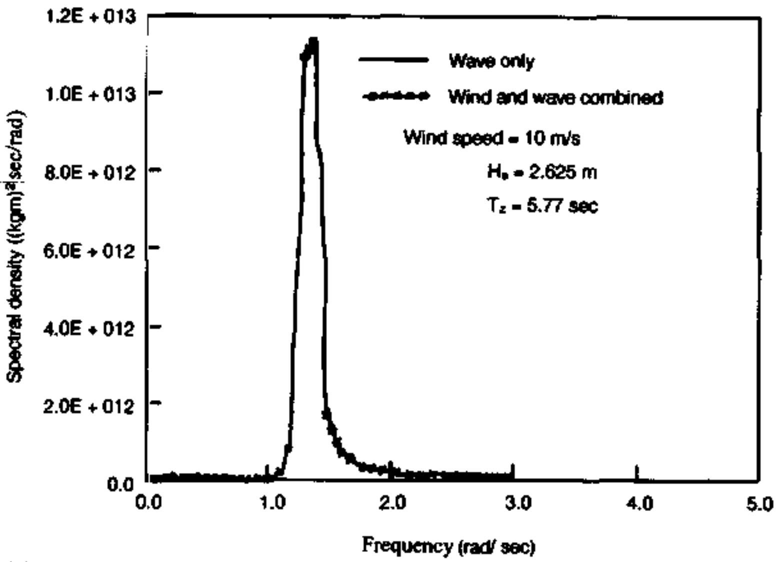

(c)

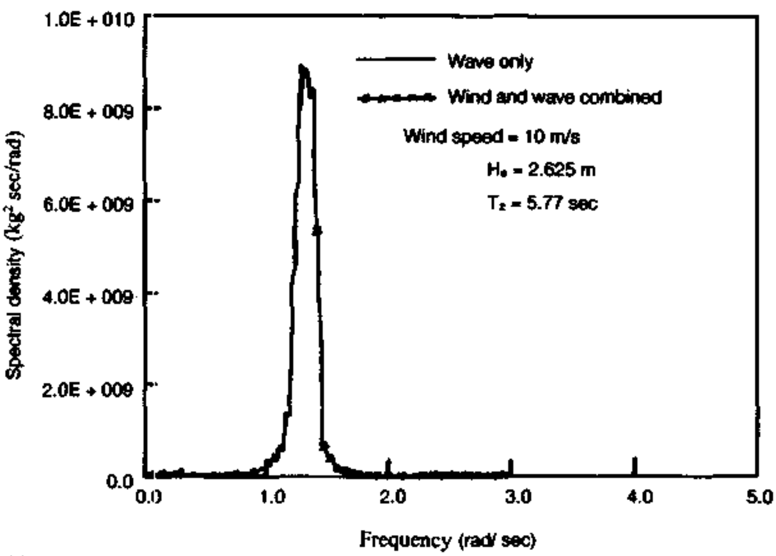

(d)

Fig. 6. Continued.

forces, ignoring the variable submergence effects due to waves. It is seen that the dynamic effect of the wind assumes significance at lower wind velocity when the wave's significant energy contents are far away from it. The standard deviation for wave and wave and wind together becomes close for higher wind velocities (or higher wave periods), the standard deviation for a wave alone being smaller.

Table 3 shows the mean and standard deviation of the response quantities for various

Table 2. Mean and standard deviation of the responses (variable submergence due to wave is neglected)

Wave and mean wind velocity	Forces	Responses	Mean	Standard deviation
2.625 m and 5.77 s	Wave	TD	0.00075545	0.03836
		GF	116.214	4808.0655
		BM	− 1028.27	1692808.005
		SF	− 78.80977	44072.5968
10 m/s	Wind + wave	TD	0.01662055	0.0465456
		GF	2547.86585	6303.88769
		BM	− 71350.60133	169319.545
		SF	− 2500.2289	44187.102
5.91 m and 8.66 s	Wave	TD	0.0036	0.15251
		GF	554.314	23516.648
		BM	− 4087.7508	2168659.33
		SF	− 314.323	57304.4605
15 m/s	Wind + wave	TD	0.033704	0.1536
		GF	5167.4135	23689.87
		BM	− 139311.7619	2165756.22
		SF	− 4897.909239	57227.6157
10.5 m and 11.546 s	Wave	TD	0.00582	0.5053376
		GF	891.1637	78427.0733
		BM	− 5306.3377	2689660.172
		SF	− 409.4228	68266.627
20 m/s	Wind + wave	TD	0.0557537	0.505816
		GF	8536.0134	78489.4897
		BM	− 231365.66896	2691802.3
		SF	− 8016.7036	68327.886
16.4 m and 14.43 s	Wave	TD	0.0255338	1.59898
		GF	3881.0917	244624.0731
		BM	− 16344.7677	4912609.576
		SF	− 1265.15488	130886.9718
25 m/s	Wind + wave	TD	0.10205	1.60125
		GF	15426.357	244940.81
		BM	− 359040.89786	4923515.005
		SF	− 12757.7891	131278.33

TD: tip displacement (m); GF: guy force (kg); BM: bending moment at guy node (kgm); SF: shear force at guy node (kg).

forces, including the effect of variable sumbergence due to waves. The standard deviation, for the smallest wave, increases for tip displacement and guy force, whereas it decreases for bending moment and shear force when the effect of variable submergence due to waves is considered in the analysis. For all other wave cases the standard deviation decreases for all the response quantities when variable submergence due to waves is considered.

4. CONCLUSIONS

The responses of an offshore guyed tower for random wind forces, wind generated random wave forces and their combination are obtained using an iterative frequency domain technique which duly considers different kinds of nonlinearities present in the hydrodynamic load. A numerical study is conducted to study the relative importance of the wind forces on the overall response of the idealised offshore guyed tower. The results of the study indicate the following.

1. Contributions of wind forces to the responses are governed by the size of the waves

Table 3. Mean and standard deviation of the responses (variable submergence due to wave is included)

Wave and mean wind velocity	Forces	Responses	Mean	Standard deviation
2.625 m and 5.77 s	Wave	TD	− 0.00265	0.04034
		GF	− 407.0677	5257.52
		BM	1042.78	1611489.66
		SF	151.407	42568.5
10 m/s	Wind + wave	TD	0.01611373	0.053848862
		GF	2469.3269077	7637.735266
		BM	− 74105.0366	1611148.66
		SF	− 2580.2777	42595.7744
5.91 m and 8.66 s	Wave	TD	− 0.000877	0.1485178
		GF	− 136.5347	22913.56276
		BM	− 18792.6385	2053544.944
		SF	− 952.26755	54799.57287
15 m/s	Wind + wave	TD	0.0351204	0.150645
		GF	5381.1823	23240.697
		BM	− 165687.4872	2050170.725
		SF	− 6243.87074	54699.177
10.5 m and 11.546 s	Wave	TD	0.0025911	0.49874
		GF	383.4081	77410.29
		BM	− 51821.80468	2548531.832
		SF	− 2884.244	65632.1654
20 m/s	Wind + wave	TD	0.0633626	0.49713
		GF	9693.55667	77143.373
		BM	− 301013.3822	2544857.56
		SF	− 11866.17945	65594.207
16.4 m and 14.43 s	Wave	TD	0.019122	1.58683
		GF	2874.83557	242756.535
		BM	− 139271.6778	4844750.086
		SF	− 7728.53	130853.2132
25 m/s	Wind + wave	TD	0.114479	1.572323
		GF	17272.0369	240538.978
		BM	− 522618.6615	4814041.96
		SF	− 21634.66374	131209.7557

generated by the wind velocity. For higher wind velocities, generating larger waves (larger periods), the contribution of wind forces to the dynamic response is insignificant due to the significant wave frequency becoming smaller and closer to the wind frequency and thereby suppressing the response caused by the wind. For smaller wind velocities, generating smaller waves (smaller periods), the contribution of wind forces to the dynamic response becomes significant, since the significant wave frequency becomes higher and moves away from the wind frequency.

2. Wind forces affect only the contribution of the first mode response for tip displacement and guy forces. They do not practically affect the bending moment and shear force, which are predominantly governed by the second mode response and the response caused by significant wave components (which are at higher frequencies than the first mode frequency).
3. The wind forces increase the mean values of the response quantities.
4. The inclusion of the effect of variable submergence due to waves decreases the standard deviation for all the response quantities for relatively higher waves.

REFERENCES

Ansari, K. A. (1991) On the design of multi-component cable systems for moored offshore vessels. *Energy Conversion and Management* **31**, 295–307.

Chakrabarti, S. K. (1971) Discussions on dynamics of single point mooring in deep water. *Journal of Waterways, Harbour and Coastal Engineering, ASCE* **97**(3), 588–590.

Davenport, A. G. (1961) The spectrum of horizontal gustiness near the ground in high winds. *Journal of Royal Meteorological Society* **87**. 194–221.

Goda, Y. (1970) Numerical experiments on wave statistics with spectral simulation. *Report of the Port and Harbour Research Institute, Japan* **9**, 16–19.

Jain, A. K. and Datta, T. K. (1990) Nonlinear response of guyed tower to random wave forces. *International Journal of Probabilistic Engineering Mechanics* **5**, 66–75.

Pierson, W. J. and Moskowitz, L. (1964) A proposed spectral form for fully developed wind seas based on the similarity theory of S. A. Kitaigorodiskii. *Journal of Geophysical Research* **69**, 5181–5190.

Qi, X.-Y., Xio, N., Cheng, T.-Y. and Qi, T. (1991) Experimental study on the behaviour of a two-tension leg buoy mooring system in wind, wave and current. Proceedings of the First International Offshore and Polar Engineering Conference, Edinburgh, pp. 266–272.

Simiu, E. and Scanlan, R. H. (1978) *Wind Effects on Structures*. John Wiley, New York.

Smith, C. E. (1990) Wind on offshore platforms. *Proceedings of the 22nd Joint Meeting of the U.S.–Japan Cooperative Program in Natural Resources – Panel on Wind and Seismic Effects*, Washington, DC. NIST Special Publication No. 796, pp. 45–50.

Vickery, P. J. (1990) Wind and wave loads on a tension leg platform. Theory and experiment. *Journal of Wind Engineering and Industrial Aerodynamics* **36**, 905–914.